
Class Conditional Gaussians for Continual Learning

Thomas L. Lee
School of Informatics
University of Edinburgh
T.L.Lee-1@sms.ed.ac.uk

Amos Storkey
School of Informatics
University of Edinburgh
a.storkey@ed.ac.uk

Abstract

Dealing with representation shift is one of the main problems in online continual learning. Current methods mainly solve this by reducing representation shift, but leave the classifier on top of the representation to slowly adapt, in many update steps, to the remaining representation shift, increasing forgetting. We propose DeepCCG, an empirical Bayesian approach to solve this problem. DeepCCG works by updating the posterior of a class conditional Gaussian classifier such that the classifier adapts instantly to representation shift. The use of a class conditional Gaussian classifier also enables DeepCCG to use a log conditional marginal likelihood loss to update the representation, which can be seen as a new type of replay. To perform the update to the classifier and representation, DeepCCG maintains a fixed number of examples in memory and so a key part of DeepCCG is selecting what examples to store, choosing the subset that minimises the KL divergence between the true posterior and the posterior induced by the subset. We demonstrate the performance of DeepCCG on a range of settings, including those with overlapping tasks which thus far have been under-explored. In the experiments, DeepCCG outperforms all other methods, evidencing its potential.

1 Introduction

Real world use of deep learning methods can often necessitate dynamic updating of solutions on non-stationary data streams [11, 3]. This is one of the main problems studied in continual learning and as a result, continual learning has become of increasing interest to the machine learning community, with many proposed approaches [30] and settings [18, 3, 8]. Currently, one of the biggest challenges in continual learning is catastrophic forgetting. *Catastrophic forgetting* describes the common occurrence in learning where unconstrained deep models easily forget information derived from previous data after updating on other data. While there have been significant steps taken to solve this problem [8, 25], in many settings there are still gains to be made [11].

The setting considered here is *online continual learning* [5, 2] where a data stream is split into a sequential set of *tasks*. Each task is encapsulated by a representative dataset (sampled i.i.d. from a task distribution) which is given to a method *batch by batch*. Different tasks will generally be associated with different distributions, as well as different target problems. Target problems are summarised in a task objective function. Here, the task objective is classification [18], where the classes being considered vary between tasks. The objective of any method, after sequentially seeing the tasks, is to perform well on all of them, given constraints on the memory used by the method.

Most continual learning methods can be seen as a composition of an encoder and classifier. The encoder maps data instances to a representation and the classifier given an example in representation space assigns a class to it. In online continual learning when the encoder is updated, the representation of data from previous tasks shift, which can lead to catastrophic forgetting. Therefore, many standard online continual learning methods aim to minimise representation shift of data from old tasks. For instance, many methods reduce representation shift by storing previous data points in a memory buffer

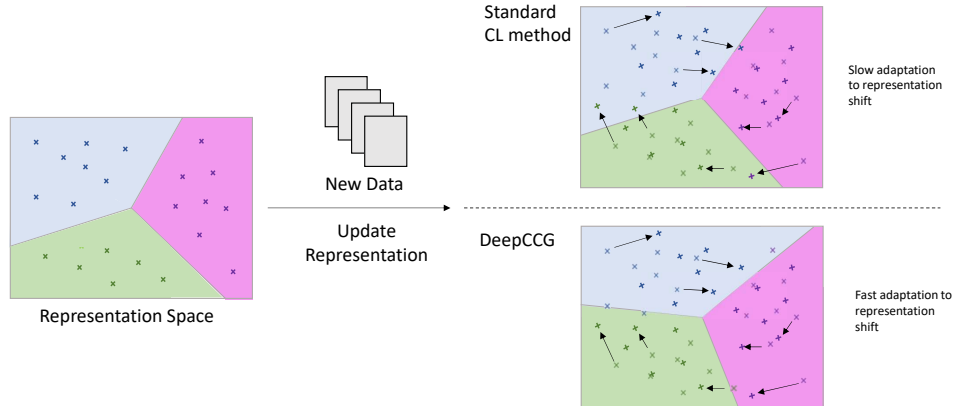


Figure 1: Diagram showing that when updating a model on new data current online continual learning methods only slowly adapt the classifier, i.e. decision boundary in representation space, to this representation shift. On the other hand, DeepCCG quickly adapts the decision boundary, improving learning as the classifier is better matched to the current representation.

and using them to regularise the update of the representation [8, 36]. However, these methods do not fully prevent representation shift (indeed doing so entirely would severely hinder model flexibility) and it takes many update steps for them to adapt their classifier to representation shift, impeding learning and causing forgetting (see Figure 1 and analysis of representation shift in Section 5.2).

The point of this paper is to identify a clean way to immediately adapt a classifier to representation shift, while at the same time enabling learning of better and better representations. To do this we propose a new method DeepCCG which leverages a Bayesian class-conditional Gaussian model for classification. The use of such a classifier has three main effects. First, the posterior of the parameters of the class-conditional model can be recomputed to instantly adjust to representation shift. This means that the classifier and the shifted representation will be better aligned, removing the potential for the representation to unnecessarily change to better fit the outdated classifier. Second, it allows for the tractable use of a conditional marginal likelihood for optimizing the parameters of the embedding function. This can be seen as a new type of replay; replay methods have been shown to reduce representation shift, increasing performance [36, 40, 8]. Third, a fixed subset of data is chosen to track representation shift, by selecting the subset that best recreates the posterior distribution. This method for selecting samples is shown to be robust to general kinds of representation shift (see Section 4) and is required for DeepCCG to perform well (see ablation study in Section 5.2).

In our experiments we look at two specific settings, the commonly used disjoint tasks setting, where each task contains different classes to any other [8] and an underexplored shifting window setting, where there is an overlap between what classes are in each task. The reason we look at a setting with an overlap between tasks is to explore each method’s ability to exploit shared information between tasks, which is a beneficial property for methods to have [4]. The results of our experiments show that DeepCCG performed best out of all methods tested, highlighting the potential of the approach.

The main contributions of this work are: 1) An online continual learning approach DeepCCG, which by learning the classifier in a tractable Bayesian manner adapts to representation shift in one step and performs best in our experiments; 2) Use of a log conditional marginal likelihood loss term to fit the embedding function, which to our knowledge is the first likelihood loss conditioned on part of the data to be used in continual learning; 3) A new method to select what samples to store in memory, by minimising the KL-divergence between the true posterior and the one induced by the subset of data to be stored in memory; 4) An unexplored experimental setting, the shifting window setting, which explores how well methods do when there is increased shared information between tasks.

2 Related work

There are three main paradigms for solving continual learning problems: *regularisation*, *parameter-isolation* and *replay* [8]. *Regularisation* methods aim to prevent catastrophic forgetting by adding terms to the loss which try to prevent the network from erasing the information of previous tasks

[21, 19]. *Parameter-Isolation* methods look at controlling what parameters of a neural network are used for what tasks and contain methods which dynamically expand neural networks [26]. Finally, *Replay* methods aim to solve continual learning problems by storing a subset of previously seen samples, which are then trained on alongside new incoming data. This is the approach our method is part of. Replay methods have been shown to have competitive if not the best performance across many settings [36, 40, 27]. The standard replay method is experience replay (ER) [7, 6, 1], which in the online setting looked at in this work, selects samples to store using reservoir sampling [38], we call this variant ER-reservoir [7]. One of the main questions to be answered by a replay-based approach is how to select what samples to store in memory. While reservoir sampling has been shown to be very effective [39] there have been other methods proposed for sample selection, for example ones which use information-theoretic criteria [39] and others maximising the diversity of the gradients of stored examples [2]. There has also been a Bayesian method proposed to select samples called InfoGS [34], which is somewhat similar to our method but only uses the probability model to select samples, not for prediction or training. Additionally, there exists methods to select what examples to replay at each update step [1, 33] which are complementary/orthogonal to this work.

There has been considerable work on using Bayesian methods in continual learning [28, 9, 23], perhaps inspired by the fact that true online Bayesian inference cannot suffer from catastrophic forgetting [28]. Bayesian perspectives have mainly been used for regularisation based methods, where a popular approach is to use variational inference [28, 12, 42]. These variational inference methods focus on the offline continual learning setting where a learner has access to all of the data of a task at the same time and, in previous work, are often limited to being used in conjunction with small neural networks, mainly due to the need to sample multiple networks when calculating the loss [16, 28]. Therefore, these methods are not suited to the settings we consider in this paper. Bayesian methods have also been used in generative replay based approaches, where instead of storing and replaying real samples they use generated pseudo-samples [32]. Generative replay methods focus on the offline scenario, where it is possible to iterate over the whole of a task’s data to fit a generator, while we look at the more realistic online scenario in this work. Finally, when it comes to replay with real examples, there has been relatively little work on using Bayesian methods, specifically for empirical Bayesian methods where there is a requirement to prevent forgetting when fitting the embedding function, which we aim to help to fill in by proposing DeepCCG.

In this work we look at two types of settings, one where the sets of class labels are disjoint between tasks and another where there is an overlap between the classes seen in each task. Disjoint tasks is a commonly explored setting [8] while having some class overlap between tasks is not often studied, but arguably is more realistic. Slightly tangential to the settings considered here, there has been some work looking at class overlap settings where blurry tasks are considered [31, 4, 2], that is when a disjoint task setting is modified by adding to each task a small number of samples sampled from any class, often around 10% of the original task’s size.

3 Online continual learning

Online continual learning is when a learner is sequentially given batches of data one by one, along with a task identifier for each batch, and cannot revisit previous batches. Different batches may be drawn from different tasks according to some unknown non-stationary process. The goal of the learner is to be able to perform well on all tasks at the end of training. We consider two cases, *task-incremental* and *class-incremental* learning, respectively corresponding to whether the learner can access task identifiers or not at test time [18, 31].

Specifically, we consider classification tasks. Let X denote a shared data space, and C denotes the set of all classes being considered. Let $t \in T$ denote a particular task, which generates data $S_t = \{(x_i, y_i) | i = 1, 2, \dots\}$, containing data instances $x_i \in X$ and labels $y_i \in C_t$, where $C_t \subset C$ are the subset of classes relevant for this task. For simplicity, we follow previous work [8] and assume the number of classes in each task is the same, i.e. $|C_t| = k, \forall t$.

The learner is provided with a temporal sequence (length N) of data batches and task identifiers $((D_j, t_{D_j}) | j = 1, 2, \dots, N)$, where j indexes batches and t_{D_j} denotes the task identifier for batch D_j . At each time step j , the batch D_j is a sample from a single task and the *task identifier* t_{D_j} determines this task, indicating the classes $C_{t_{D_j}}$ which are relevant for that task. We use the notation $D_{<j}$ to denote $\{D_1, D_2, \dots, D_{j-1}\}$, the data from all batches seen prior to the time step j .

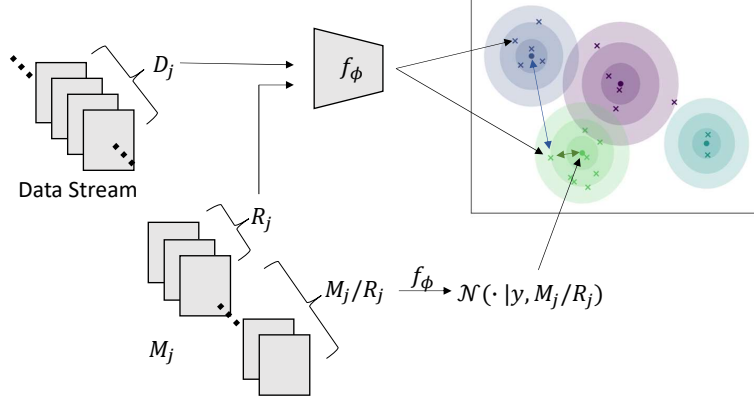


Figure 2: Diagram of DeepCCG’s training routine. At time j the learner is given a sample of data D_j and has a memory of stored datapoints M_j . The memory is randomly split into replay data R_j and the rest M_j/R_j . Learning happens by taking a gradient step on the parameters of the embedding function ϕ using a log conditional marginal likelihood function over D_j and R_j , where M_j/R_j is used to induce a posterior over the means of the per-class Gaussians and so define the conditional marginal likelihood function used. Therefore, training aims to move the data points into per-class clusters, by drawing the embedded examples of D_j and R_j towards their own class means and away from the other class means, as shown by the coloured arrows in the figure.

Algorithm 1 DeepCCG update step at time j

input D_j (training batch), t_{D_j} (task identifier for batch), M_j (memory), f_{ϕ_j} (embedding function)

Update class-conditional Gaussian classifier and embedding function:

$R_j = \text{UniformSample}(M_j)$

Calculate posterior of class-conditional Gaussian classifier: $p(\mu_c | M_j/R_j)$ for each class c

Calculate $\log(p(y|z = f_{\phi_j}(x), t_{(x,y)}, M_j/R_j))$ using Eq. 6 and posteriors $p(\mu_c | M_j/R_j)$

Update embedding function: $\phi_{j+1} = \phi_j + \eta \nabla_{\phi} \sum_{(x,y) \in D_j \cup R} \log(p(y|z = f_{\phi_j}(x), t_{(x,y)}, M_j/R_j))$

Update memory:

for each class c in M_j **do**

 initialise β

for 1 to B **do**

$\beta \leftarrow \beta + \eta \nabla_{\beta} \mathcal{L}(\beta; D_{j,c}, M_{j,c})$, where $\mathcal{L}(\beta; D_{j,c}, M_{j,c})$ is defined in Eq. 11

end for

 Set M_{j+1} to be the set of samples, with their task identifiers, with the m largest β values

end for

During training, the learner receives each batch in sequential order; after training on a batch the learner must discard all the data it does not store in its fixed-size memory buffer. At test time, the learnt model is given an unseen test set from all the classes seen during training and is provided with task identifiers in the task-incremental learning scenario or without in the class-incremental learning scenario. This experimental setup is commonly used in the continual learning literature [5, 31].

4 Deep class conditional Gaussians

We propose an empirical Bayesian method, DeepCCG, to approach the online continual learning problem. DeepCCG consists of three main parts. Firstly, a class-conditional Gaussian classifier is used on top of a neural network embedding function. The classifier is learnt using in a Bayesian manner, where by recomputing its posterior it adjusts instantly to representation shift. Secondly, DeepCCG’s embedding function is learnt using a log conditional marginal likelihood loss which minimises unnecessary representation shift. The loss used to learn the embedding function calculates the learnt classifier and so the learning of the whole method can be seen as end-to-end. Finally, DeepCCG uses a new method based on minimising information loss to select a subset of examples to store in memory, these examples are needed when updating both the classifier and the embedding function, to model and reduce representation shift. The sample selection mechanism is shown to be

robust to certain kinds of representation shift. These three parts are described in detail below and additionally a pseudocode description of the learning of DeepCCG is presented in Algorithm 1.

Probabilistic classifier The probabilistic model of DeepCCG is defined as follows. Let Z denote a representation space. We assume that we have a neural network embedding function $f_\phi : X \rightarrow Z$ and a fixed memory of size m . The memory buffer stores as one element an example (x, y) and its associated task identifier $t_{(x,y)}$ —in common with previous work [5]. We define a class-conditional Gaussian model in the representation space Z ,

$$y|t \sim \text{Cat}(C_t, (1/|C_t|)\mathbf{1}) \quad (1)$$

$$z|y \sim \mathcal{N}(\mu_y, \mathbf{I}) \quad (2)$$

$$\mu_y \sim \mathcal{N}(\mathbf{0}, \mathbf{V}_0), \quad (3)$$

where t is a given task identifier, $z = f_\phi(x)$, $\{\mu_y|y \in C\}$ are the parameters of the classifier being the per-class means in Z and $\text{Cat}(C_t, (1/|C_t|)\mathbf{1})$ is the uniform categorical distribution over the classes of task t . We choose $\mathbf{V}_0 = a\mathbf{I}$, where in practice we take $a \rightarrow \infty$. We do not specify a model where the covariance matrix is also a parameter as we learn the embedding function, hence the case of a global shared covariance is implicitly covered through learning a linear remapping to a fixed covariance, meaning we do not lose flexibility by assuming fixed covariances. The probabilistic classifier is defined as the posterior predictive distribution of the model, given some data D ,

$$p(y|x, t_{(x,y)}, D) = \int p(y|z = f_\phi(x), t_{(x,y)}, \theta = \{\mu_c|c \in C\})p(\theta = \{\mu_c|c \in C\}|D)d\theta, \quad (4)$$

where

$$p(y|z = f_\phi(x), t_{(x,y)}, \theta = \{\mu_c|c \in C\}) = \frac{p(z|y, \mu_y)p(y|t_{(x,y)})}{\sum_{c \in C} p(z|c, \mu_c)p(c|t_{(x,y)})}. \quad (5)$$

We assume the labels are conditionally independent given the task, the per-class means $\{\mu_c|c \in C\}$ and the data instances (each an element of X) and that z is independent of the task given its class y .

To learn the classifier, DeepCCG needs to compute the posterior of the per-class means, while being able to adapt to representation shift. The posterior is tractable and easy to compute in one step, as shown in Appendix D Eq. 13, as we use a class-conditional Gaussian model and a conjugate prior for the per-class means, which is the main reason we use this model along with its good performance when used on top of neural network embeddings [29, 15]. If f_ϕ is fixed, so there is no representation shift, we can update our beliefs about the per-class means on seeing batch D_j and its task identifier t_{D_j} by simply using Bayes rule, calculating the posterior $p(\{\mu_c|c \in C\}|D_j, D_{<j})$. However, in our setting, we need to update f_ϕ continually and so there is representation shift, which changes the value of $p(\{\mu_c|c \in C\}|D_j, D_{<j})$. We cannot recompute $p(\{\mu_c|c \in C\}|D_j, D_{<j})$ as we are unable to store all the previous examples in memory. Therefore, DeepCCG stores in memory a set of representative examples M with which we can compute an approximate posterior $p(\{\mu_c|c \in C\}|M)$ after a change in f_ϕ . It is important to note that we can compute this posterior in one step and hence that we can quickly adapt the classifier to representation shift, reducing forgetting and improving learning as the classifier and representation are better matched.

Learning the embedding DeepCCG uses an empirical Bayesian procedure to update the embedding function f_ϕ , that is, it uses a novel log conditional marginal likelihood loss term. At time j , in response to the arrival of batch D_j , with task identifier t_{D_j} , and having received the memory buffer M_j , DeepCCG takes the following steps to update the embedding function (shown in Figure 2). First, it selects a random set $R_j \subset M_j$, of size r , from the memory buffer to replay. Then it calculates the output of the classifier for each example $(x, y) \in D_j \cup R_j$, which is the posterior predictive distribution $p(y|f_{\phi_j}(x), t_{(x,y)}, M_j/R_j)$, conditioning on the rest of the examples M_j/R_j and where ϕ_j are the current parameters of the embedding function and $t_{(x,y)}$ is the task identifier for the example. The posterior predictive distributions are calculated using the embedded data instances and the posterior of the per-class means. It can be shown to be, by using Eq. 4 (see Appendix D for the derivation):

$$p(y|z = f_{\phi_j}(x), t_{(x,y)}, M_j/R_j) = \frac{\mathcal{N}\left(z|\overline{M_{j,y}^Z/R_j^Z}, \left(1 + \frac{1}{m-r}\right)\mathbf{I}\right)}{\sum_{c \in C_{t_{(x,y)}}} \mathcal{N}\left(z|\overline{M_{j,c}^Z/R_j^Z}, \left(1 + \frac{1}{m-r}\right)\mathbf{I}\right)} \quad (6)$$

where $M_{j,y}^Z = \{f_{\phi_j}(x)|(x, y') \in M_j \wedge y' = y\}$ are the embeddings of samples in the memory buffer of class y . R_j^Z is defined likewise and we use the notation \overline{S} to denote the mean of the elements of a

set S . As in meta-learning [13, 17], the posterior predictive distributions are used as a fixed likelihood term for each individual unseen data item. This leads to a conditional log-marginal likelihood as the objective in DeepCCG’s embedding update rule:

$$\phi_{j+1} = \phi_j + \eta \nabla_{\phi} \sum_{(x,y) \in D_j \cup R_j} \log(p(y|z = f_{\phi_j}(x), t_{(x,y)}, M_j/R_j)). \quad (7)$$

The reason DeepCCG uses a conditional log-marginal likelihood loss is because conditioning the likelihood on some examples M_j/R_j stabilises the output of the probabilistic classifier and hence the loss term used. This is because by conditioning the marginal likelihood on M_j/R_j , the posterior DeepCCG averages over is more informative than using the unconditioned prior, having some belief of where the position of embedded data instances should be and so provides a better signal to fit the embedding function. Additionally by replaying the examples R_j , treating them like new data, the loss leverages a new type of replay, where performing replay is widely known to be effective at reducing forgetting and minimising unnecessary representation shift [36, 40, 27].

Sample selection A key component to DeepCCG is how to select samples to store in the memory buffer. We focus on ensuring the least amount of information is lost about the position of the per-class means of the class conditional Gaussian classifier, after a shift in representation. Hence, because all the information available to inform the value of the classifiers per-class mean parameters is encapsulated in the full posterior over the seen data, we target choosing a set of memory samples that best recreate that posterior, preventing as much information loss as possible. Therefore, to perform sample selection we minimise the KL divergence between two posterior distributions: the posterior over parameters induced by the new memory being optimized, and the posterior induced by the current batch and the old memory. We keep the number of samples in memory for each class balanced, so minimising the KL divergence is equivalent to minimising the per-class KL divergence which reduces to the squared Euclidean distance between the means of a class’s embedded data. Formally, we select the new memory using,

$$M_{j+1,y} = \arg \min_{M'_y} (\text{KL}(p(\mu_y | D_{j,y}, M_{j,y}) \| p(\mu_y | M'_y))) \quad (8)$$

$$= \arg \min_{M'_y} (\| \overline{D_{j,y}^Z \cup M_{j,y}^Z} - \overline{M_y'^Z} \|_2^2), \quad (9)$$

where $M'_y \subseteq (D_{j,y} \times \{t_{D_j}\}) \cup M_{j,y}$, $M_{j+1,y}$ is the new memory to be selected for class y , $M_{j,y}$ is the set of samples of class y in memory when receiving the current batch of data and $D_{j,y}$ is the set of samples of class y in the current batch. Importantly, this sample selection mechanism is robust to representation shift, when modeled as an additive i.i.d. change in representation. This is because, given the shifted representations $z^* = z + \epsilon_z$, where $z \in D^Z \cup M^Z$ and ϵ_z is i.i.d. sampled from an arbitrary distribution with bounded mean and variance, we have that (proved in Appendix E):

$$\mathbb{E}[\text{KL}(p(\mu_y | D_{j,y}^{Z*}, M_{j,y}^{Z*}) \| p(\mu_y | M_y'^{Z*})))] = \| \overline{D_{j,y}^Z \cup M_{j,y}^Z} - \overline{M_y'^Z} \|_2^2 + \nu \left(\frac{1}{|M_y'^Z|} - \frac{1}{|D_{j,y}^Z \cup M_{j,y}^Z|} \right), \quad (10)$$

where the expectation is taken over the additive shift terms ϵ , ν is the sum over the per-dimension variances of the shift distribution, $D_{j,y}^{Z*} = \{z^* = z + \epsilon_z | z \in D_{j,y}^Z\}$ and $M_{j,y}^{*Z}$ is defined likewise. Therefore, in expectation, the samples selected to be stored in memory after a shift in representation are still the best samples to store in memory, in terms of preserving posterior information. Hence, our sample selection mechanism is robust to this type of representation shift.

Performing the minimization in Eq. 9 is computationally hard, so we utilise a relaxation of the problem using *lasso* [14], whereby our method selects the new memory by assigning to each embedded input z_i a zero-to-one weight β_i and performing gradient descent on the loss

$$\mathcal{L}(\beta; D_{j,y}, M_{j,y}) = \| \overline{D_{j,y}^Z \cup M_{j,y}^Z} - \frac{1}{\|\beta\|_1} \sum_{i | (x_i, y_i) \in D_{j,y} \cup M_{j,y}} \beta_i z_i \|_2^2 + \lambda \|\beta\|_1. \quad (11)$$

Then, after termination, our method selects the m examples with the largest weights to be the examples stored in memory, where they are stored along with their task identifiers.

5 Experiments

5.1 Experimental setup

Benchmarks In our experiments we look at task and class incremental learning in both the disjoint tasks and shifting window settings. Furthermore, we consider three different datasets: CIFAR-100 [22], MiniImageNet [37] and CIFAR-10 [22], where both CIFAR-100 and MiniImageNet contain 100 classes, while CIFAR-10 contains 10 classes. For disjoint tasks, we split data evenly across a certain number of tasks while assigning all samples with a particular class to only one task—this is often called the ‘split tasks’ setting in previous work [8, 5]. We split CIFAR-10 into 5 tasks where there are 2 classes per task and for CIFAR-100 and MiniImageNet we split the dataset into 20 tasks with 5 classes per task. In the alternative shifting window setting, we split the datasets up into tasks by fixing an ordering of the classes c_1, \dots, c_k and construct the t th task by selecting a set of samples from classes c_t, \dots, c_{t+l} , where l is the window length. No two tasks contain the same example and each task has the same number of samples per-class. For CIFAR-10 we use a window length of 2 and for CIFAR-100 and MiniImageNet we use a window length of 5. Additionally, for all experiments we train with 500 samples per-class. We evaluate the methods using a standard metric for continual learning, average accuracy[5]. The average accuracy of a method is the mean accuracy on a reserved set of test data across all tasks after training on all tasks.

Methods We compare DeepCCG to representative methods of the main paradigms of continual learning. For regularisation methods we compare against a fixed memory variant of EWC [19, 21]; for parameter-isolation methods we compare to PackNet [26], but only in the task-incremental setting as it requires task identifiers at test time. For replay methods, which includes DeepCCG, we compare against ER-Reservoir [7], A-GEM [5], EntropySS [39], and GSS [2]; EntropySS and GSS are different memory sample selection strategies for ER. When training, all methods are given task identifiers which state what classes are in a task. Task identifiers are also given at test time in the task-incremental scenario while in class-incremental learning the task-identifier at test time is treated as stating a data instance can belong to any class. We also compare against two baselines: SGD which is when learning is performed using SGD with no modification and Multi-Task which is an upper bound and is when we learn the base neural network offline—with task identifiers for the task-incremental experiments and without for the class-incremental experiments. All methods use the same embedding network for all experiments which is a ResNet18 with six times fewer filters and Instance Normalisation [35] instead of Batch Normalisation layers [20], which is similar to other work [27, 10]. A batch size of 10 is used throughout, with all replay methods having a replay size of 10. A memory size of 10 samples per-class is used for the task-incremental setting, and 30 for the harder class-incremental setting. Further experimental details are provided in Appendix F.

5.2 Results

In the task-incremental experiments, we see from Table 1 that DeepCCG performs the best out of the methods compared. For example, DeepCCG on CIFAR-100 achieves mean average accuracies of 56.62% and 60.46% for the shifting window and disjoint tasks settings, respectively, which are 2.57% and 2.15% better than any other method. ER-reservoir and GSS are the next best performing methods, which alternate in achieving the second best performance in the task-incremental experiments, except for the results on MiniImageNet in the disjoint tasks setting where EntropySS performs second best. This shows that which memory selection method for experience replay is best depends on the dataset and setting, with not one performing always better than the rest. Overall, DeepCCG had an average performance improvement of 2.145% over the other methods in the task-incremental experiments, this shows that DeepCCG performs well in the task-incremental scenario where, especially for the disjoint tasks setting, it is hard to get large performance improvements [31].

For the experiments on class-incremental learning, we see that DeepCCG performs well, outperforming the other methods. The results of the class-incremental experiments are shown in Table 2 and displays for instance that DeepCCG on CIFAR-100 achieves mean average accuracies of 18.00% and 17.32% on the shifting window and disjoint tasks settings, respectively. The performance of DeepCCG on CIFAR-100 are 10.40% and 9.45% better than any other method. Overall, DeepCCG across all datasets and settings in class-incremental learning has an average performance improvement of 7.72%, which shows that the method performs well and with the results on task-incremental learning shows that DeepCCG is effective in both scenarios. Also, it is interesting to note that DeepCCG per-

Table 1: Results of task-incremental learning experiments on CIFAR-10, CIFAR-100 and MiniImageNet, where SW and DT stand for the shifting window and disjoint tasks settings, respectively. We report mean average accuracy with their standard errors across three independent runs.

Method	CIFAR-10		CIFAR-100		MiniImageNet	
	SW	DT	SW	DT	SW	DT
EWC	58.68 \pm 1.88	63.33 \pm 0.87	36.65 \pm 1.07	42.39 \pm 0.79	32.42 \pm 1.13	29.57 \pm 0.69
PackNet	69.29 \pm 2.27	66.97 \pm 1.47	40.21 \pm 0.96	50.28 \pm 0.58	34.15 \pm 1.28	37.86 \pm 1.71
ER-reservoir	70.44 \pm 0.81	66.71 \pm 0.90	54.05 \pm 0.63	58.31 \pm 1.08	41.04 \pm 1.54	40.29 \pm 1.08
A-GEM	57.63 \pm 2.16	57.28 \pm 2.61	29.01 \pm 1.45	39.00 \pm 0.75	26.97 \pm 1.26	30.08 \pm 1.86
EntropySS	67.93 \pm 0.63	64.96 \pm 0.91	51.80 \pm 0.70	56.75 \pm 0.81	40.03 \pm 0.61	41.12 \pm 0.51
GSS	71.55 \pm 1.45	67.30 \pm 1.27	48.20 \pm 0.33	49.92 \pm 0.50	37.91 \pm 0.49	38.77 \pm 0.98
DeepCCG (ours)	74.65\pm2.00	69.29\pm0.89	56.62\pm0.29	60.46\pm0.24	42.18\pm0.45	43.04\pm0.64
SGD	63.21 \pm 2.09	63.58 \pm 0.31	35.63 \pm 1.27	42.50 \pm 1.40	33.23 \pm 0.67	31.61 \pm 0.70
Multi-Task (UB)	96.20 \pm 0.69	73.37 \pm 1.82	90.42 \pm 1.87	59.76 \pm 0.49	89.81 \pm 0.25	48.46 \pm 1.21

Table 2: Results of class-incremental learning experiments on CIFAR-10, CIFAR-100 and MiniImageNet, where SW and DT stand for the shifting window and disjoint tasks settings, respectively. We report mean average accuracy with their standard errors across three independent runs.

Method	CIFAR-10		CIFAR-100		MiniImageNet	
	SW	DT	SW	DT	SW	DT
EWC	14.36 \pm 1.64	13.85 \pm 2.17	3.77 \pm 0.39	4.51 \pm 0.19	2.73 \pm 0.21	2.84 \pm 0.19
ER-reservoir	18.96 \pm 1.18	16.29 \pm 0.75	7.76 \pm 0.91	7.19 \pm 0.56	5.93 \pm 1.05	5.15 \pm 0.22
A-GEM	11.98 \pm 0.82	14.88 \pm 0.52	1.92 \pm 0.04	3.01 \pm 0.13	1.21 \pm 0.16	1.83 \pm 0.04
EntropySS	8.93 \pm 1.11	15.69 \pm 0.78	5.85 \pm 0.47	7.87 \pm 0.71	2.93 \pm 0.45	5.63 \pm 0.40
GSS	16.11 \pm 1.23	17.61 \pm 0.30	6.34 \pm 0.20	5.18 \pm 0.44	4.52 \pm 0.25	4.84 \pm 0.16
DeepCCG (ours)	26.87\pm0.47	24.27\pm0.44	18.00\pm0.72	17.32\pm0.27	11.71\pm0.39	11.88\pm0.71
SGD	13.59 \pm 1.76	13.76 \pm 1.22	4.09 \pm 0.14	3.93 \pm 0.29	1.28 \pm 0.06	2.14 \pm 0.22
Multi-Task (UB)	40.57 \pm 2.33	40.57 \pm 2.33	20.22 \pm 0.42	20.22 \pm 0.42	12.41 \pm 0.69	12.41 \pm 0.69

forms better, in terms of performance improvement over the other methods, in the class-incremental experiments than the task-incremental experiments, achieving an average performance improvement of 2.145% in task-incremental learning and 7.72% in class incremental learning. This finding is surprising as in DeepCCG there is no interaction between the mean parameters of classes which do not appear together in a training task. Therefore, these non-interacting mean parameters could be close together, harming performance in class-incremental learning, but this does not seem to be the case in practice and improving upon this is a direction for future work.

Shifting window setting The results on the shifting window setting show that current methods do not exploit the increased task overlap in the setting and hence do not utilize the increased ability to transfer knowledge between tasks. This is shown in the results as the performance of the methods are very similar between the shifting window and disjoint tasks settings; while, in the task-incremental experiments, the difference between the multi-task upper bound’s performance and the methods is much larger in the shifting window setting than that for the disjoint tasks setting.¹ This suggests that current methods do not perform between-task transfer well and so in settings of increased task overlap, where between-task knowledge transfer is more beneficial, current methods do not achieve accuracies near to that which is possible. Therefore, in these settings, where similar tasks are located temporally near to each other, a common real world property, there is a large space for new continual learning methods to be proposed which can more effectively perform between-task transfer.

¹In the class-incremental experiments the multi-task upper bound does not use task identifiers, hence we can only observe the differences in upper bound performance in the task-incremental experiments.

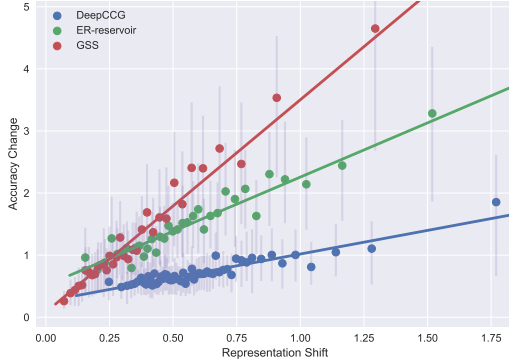


Figure 3: Binned scatter plot showing for the Mini-ImageNet disjoint tasks setting the change in accuracy against the mean change in representation after learning on a batch for the test data of the first task.

Table 3: Results of performing an ablation on DeepCCG, where we report results on DeepCCG using reservoir sampling instead of its own sample selection method (DeepCCG-reservoir), when we replace the class-conditional Gaussian model with a standard classifier head (DeepCCG-standardHead) and when we do both modifications, in which case our method reduces to the ER-reservoir method. We report the mean average accuracy with their standard errors across three independent runs on the CIFAR-100 shifting window setting using task-incremental learning.

Method	Average Accuracy
ER-reservoir	54.05 \pm 0.626
DeepCCG-reservoir	49.95 \pm 0.743
DeepCCG-standardHead	44.05 \pm 0.264
DeepCCG	56.62 \pm 0.288

Analysis of representation shift As part of our experiments we assess how well DeepCCG’s classifier update adapts to representation shift compared to other methods, showing that DeepCCG’s performance is more stable with respect to representation shift. To measure representation shift, after learning on the first task and for each incoming batch of data, we recorded the mean distance over the first task’s test data between its representation before and after updating on the incoming batch. Additionally, we measure the change in accuracy on first task’s test data before and after updating the method on the incoming batch. We present these results for task-incremental learning on MiniImageNet in Figure 3, displaying the best performing methods from our experiments. We also recorded results for EntropySS but as they were very similar to ER-reservoirs we do not include them in the figure to aid clarity; instead they are shown in Appendix G.2. Figure 3 shows that for the same amount of representation shift DeepCCG’s accuracy changes less than the other methods, as its line of best fit is the least steep. This demonstrates that the classifier of DeepCCG is more robust and better adapts to representation shift, validating DeepCCG’s use of a Bayesian classifier which in one step adapts to representation shift.

Ablation study One way to view DeepCCG is as a relative of ER-reservoir, where the methods differ in the sample selection mechanism used and the type and learning of the probabilistic classifier and embedding function. Therefore, to analyse DeepCCG, we perform an ablation, creating two adaptations of our method, DeepCCG-reservoir and DeepCCG-standardHead, by changing components of DeepCCG to what they are in ER-reservoir. DeepCCG-reservoir is when we select samples to store in memory using reservoir sampling. DeepCCG-standardHead is when we replace the class conditional Gaussian model with a standard output head (a fully connected layer, then a softmax) and learn the embedding function using the standard ER loss, while still using DeepCCG’s sample selection method. The results for the ablation are presented in Table 3 and show that both DeepCCG-reservoir and DeepCCG-standardHead perform much worse than DeepCCG. Therefore, we have shown that all of DeepCCG’s novel components are needed in conjunction for DeepCCG to perform well. We also perform an ablation on the size of memory in Appendix G.1, where we show that DeepCCG performs the best over all the memory sizes tested on.

6 Conclusions

In this work we have demonstrated that using a replay-based empirical Bayesian procedure, DeepCCG, for online continual learning is a promising direction, reducing the effect of representation shift when training. A key part of DeepCCG is to select samples to store in memory by approximately selecting the best subset that minimises the KL divergence between the posterior induced by all the currently accessible data and the posterior induced by the subset. This sample selection mechanism was found to be robust to general types of representation shift. The results show that DeepCCG performs well for online continual learning, outperforming all other methods in the commonly used disjoint tasks setting [18] as well as the under-explored shifting window setting, where there is an increased overlap between the tasks. For future work, potential directions would be to look at applying this approach to other probabilistic models and applying it to settings with imbalanced and/or noisy data [34, 41, 2].

Acknowledgments and Disclosure of Funding

References

- [1] Rahaf Aljundi, Lucas Caccia, Eugene Belilovsky, Massimo Caccia, Min Lin, Laurent Charlin, and Tinne Tuytelaars. Online Continual Learning with Maximal Interfered Retrieval. In *Proceedings of the 33rd Conference on the Advances in Neural Information Processing Systems*, pages 11849–11860, 2019.
- [2] Rahaf Aljundi, Min Lin, Baptiste Goujaud, and Yoshua Bengio. Gradient Based Sample Selection for Online Continual Learning. In *Proceedings of the 33rd Conference on the Advances in Neural Information Processing Systems*, pages 11816–11825, 2019.
- [3] Antreas Antoniou, Massimiliano Patacchiola, Mateusz Ochal, and Amos Storkey. Defining Benchmarks for Continual Few-shot Learning. *arXiv preprint arXiv:2004.11967*, 2020.
- [4] Jihwan Bang, Heesu Kim, YoungJoon Yoo, Jung-Woo Ha, and Jonghyun Choi. Rainbow Memory: Continual Learning with a Memory of Diverse Samples. In *Proceedings of the 2021 IEEE/CVF Conference on Computer Vision and Pattern Recognition*, pages 8218–8227, 2021.
- [5] Arslan Chaudhry, Marc’ Aurelio Ranzato, Marcus Rohrbach, and Mohamed Elhoseiny. Efficient Lifelong Learning with A-GEM. In *Proceedings of the 7th International Conference on Learning Representations*, 2019.
- [6] Arslan Chaudhry, Marcus Rohrbach, Mohamed Elhoseiny, Thalaiyasingam Ajanthan, Puneet K Dokania, Philip HS Torr, and Marc’ Aurelio Ranzato. On Tiny Episodic Memories in Continual Learning. *arXiv preprint arXiv:1902.10486*, 2019.
- [7] Arslan Chaudhry, Naeemullah Khan, Puneet Dokania, and Philip Torr. Continual Learning in Low-rank Orthogonal Subspaces. In H. Larochelle, M. Ranzato, R. Hadsell, M.F. Balcan, and H. Lin, editors, *of the 34th Conference on the Advances in Neural Information Processing Systems*, volume 33, pages 9900–9911, 2020.
- [8] Matthias Delange, Rahaf Aljundi, Marc Masana, Sarah Parisot, Xu Jia, Ales Leonardis, Greg Slabaugh, and Tinne Tuytelaars. A Continual Learning Survey: Defying Forgetting in Classification Tasks. *IEEE Transactions on Pattern Analysis and Machine Intelligence*, 2021. doi: 10.1109/TPAMI.2021.3057446.
- [9] Sayna Ebrahimi, Mohamed Elhoseiny, Trevor Darrell, and Marcus Rohrbach. Uncertainty-guided Continual Learning with Bayesian Neural Networks. In *Proceedings of the 8th International Conference on Learning Representations*, 2020.
- [10] Mehrdad Farajtabar, Navid Azizan, Alex Mott, and Ang Li. Orthogonal Gradient Descent for Continual Learning. *arXiv preprint arXiv:1910.07104*, 2019.
- [11] Sebastian Farquhar and Yarin Gal. Towards Robust Evaluations of Continual Learning. *arXiv preprint arXiv:1805.09733*, 2018.
- [12] Sebastian Farquhar and Yarin Gal. A Unifying Bayesian View of Continual Learning. *arXiv preprint arXiv:1902.06494*, 2019.
- [13] Marta Garnelo, Dan Rosenbaum, Christopher Maddison, Tiago Ramalho, David Saxton, Murray Shanahan, Yee Whye Teh, Danilo Rezende, and S. M. Ali Eslami. Conditional Neural Processes. In *Proceedings of the 35th International Conference on Machine Learning*, volume 80 of *Proceedings of Machine Learning Research*, pages 1704–1713, 2018.
- [14] Trevor Hastie, Robert Tibshirani, and Jerome H Friedman. *The Elements of Statistical Learning: Data Mining, Inference, and Prediction*. Springer, 2nd edition, 2009.
- [15] Tyler L Hayes and Christopher Kanan. Lifelong machine learning with deep streaming linear discriminant analysis. In *Proceedings of the IEEE/CVF conference on computer vision and pattern recognition workshops*, pages 220–221, 2020.

- [16] Christian Henning, Maria Cervera, Francesco D' Angelo, Johannes von Oswald, Regina Traber, Benjamin Ehret, Seijin Kobayashi, Benjamin F. Grewe, and João Sacramento. Posterior Meta-Replay for Continual Learning. In *Proceedings of the 35th conference on the Advances in Neural Information Processing Systems*, pages 14135–14149, 2021.
- [17] Timothy M Hospedales, Antreas Antoniou, Paul Micaelli, and Amos J Storkey. Meta-Learning in Neural Networks: A Survey. *IEEE Transactions on Pattern Analysis and Machine Intelligence*, 2021. doi: 10.1109/TPAMI.2021.3079209.
- [18] Yen-Chang Hsu, Yen-Cheng Liu, Anita Ramasamy, and Zsolt Kira. Re-evaluating Continual Learning Scenarios: A Categorization and Case for Strong Baselines. In *Proceedings of the 3rd Continual Learning Workshop, at the 32nd Conference on the Advances in Neural Information Processing Systems*, 2018.
- [19] Ferenc Huszár. Note on the Quadratic Penalties in Elastic Weight Consolidation. *Proceedings of the National Academy of Sciences*, 115(11):E2496–E2497, 2018. doi: 10.1073/pnas.1717042115.
- [20] Sergey Ioffe and Christian Szegedy. Batch Normalization: Accelerating Deep Network Training by Reducing Internal Covariate Shift. In *Proceedings of the 32nd International Conference on Machine Learning*, volume 37 of *Proceedings of Machine Learning Research*, pages 448–456, 2015.
- [21] James Kirkpatrick, Razvan Pascanu, Neil Rabinowitz, Joel Veness, Guillaume Desjardins, Andrei A Rusu, Kieran Milan, John Quan, Tiago Ramalho, Agnieszka Grabska-Barwinska, et al. Overcoming Catastrophic Forgetting in Neural Networks. *Proceedings of the national academy of sciences*, 114(13):3521–3526, 2017.
- [22] Alex Krizhevsky. Learning Multiple Layers of Features from Tiny Images. *Preprint*, 2009.
- [23] Richard Kurl, Botond Cseke, Alexej Klushyn, Patrick van der Smagt, and Stephan Günnemann. Continual Learning with Bayesian Neural Networks for Non-Stationary Data. In *Proceedings of the 8th International Conference on Learning Representations*, 2020.
- [24] Sanae Lotfi, Pavel Izmailov, Gregory Benton, Micah Goldblum, and Andrew Gordon Wilson. Bayesian Model Selection, the Marginal Likelihood, and Generalization. *arXiv preprint arXiv:2202.11678*, 2022.
- [25] Zheda Mai, Ruiwen Li, Jihwan Jeong, David Quispe, Hyunwoo Kim, and Scott Sanner. Online Continual Learning in Image Classification: An Empirical Survey. *arXiv preprint arXiv:2101.10423*, 2021.
- [26] Arun Mallya and Svetlana Lazebnik. PackNet: Adding Multiple Tasks to a Single Network by Iterative Pruning. In *Proceedings of the 2018 IEEE Conference on Computer Vision and Pattern Recognition*, pages 7765–7773, 2018.
- [27] Seyed Iman Mirzadeh, Mehrdad Farajtabar, Razvan Pascanu, and Hassan Ghasemzadeh. Understanding the Role of Training Regimes in Continual Learning. In *Proceedings of the 33rd conference on the Advances in Neural Information Processing Systems*, pages 7308–7320, 2020.
- [28] Cuong V. Nguyen, Yingzhen Li, Thang D. Bui, and Richard E. Turner. Variational Continual Learning. In *International Conference on Learning Representations*, 2018.
- [29] Oleksiy Ostapenko, Timothee Lesort, Pau Rodríguez, Md Rifat Arefin, Arthur Douillard, Irina Rish, and Laurent Charlin. Foundational models for continual learning: An empirical study of latent replay. *arXiv preprint arXiv:2205.00329*, 2022.
- [30] German I. Parisi, Ronald Kemker, Jose L. Part, Christopher Kanan, and Stefan Wermter. Continual Lifelong Learning with Neural Networks: A review. *Neural Networks*, 113:54 – 71, 2019. ISSN 0893-6080.
- [31] Ameya Prabhu, Philip HS Torr, and Puneet K Dokania. GDumb: A Simple Approach that Questions our Progress in Continual Learning. In *Proceeding of the 16th European Conference on Computer Vision*, pages 524–540, 2020.

- [32] Dushyant Rao, Francesco Visin, Andrei Rusu, Razvan Pascanu, Yee Whye Teh, and Raia Hadsell. Continual Unsupervised Representation Learning. In *Proceedings of the 33rd Conference on the Advances in Neural Information Processing Systems*, 2019.
- [33] Dongsub Shim, Zheda Mai, Jihwan Jeong, Scott Sanner, Hyunwoo Kim, and Jongseong Jang. Online Class-Incremental Continual Learning with Adversarial Shapley Value. In *Proceedings of the 35th AAAI Conference on Artificial Intelligence*, 2021.
- [34] Shengyang Sun, Daniele Calandriello, Huiyi Hu, Ang Li, and Michalis Titsias. Information-Theoretic Online Memory Selection for Continual Learning. In *Proceedings of the 10th International Conference on Learning Representations*, 2022.
- [35] Dmitry Ulyanov, Andrea Vedaldi, and Victor Lempitsky. Instance Normalization: the Missing Ingredient for Fast Stylization. *arXiv preprint arXiv:1607.08022*, 2016.
- [36] Gido M van de Ven and Andreas S Tolias. Three Scenarios for Continual Learning. *arXiv preprint arXiv:1904.07734*, 2019.
- [37] Oriol Vinyals, Charles Blundell, Timothy Lillicrap, and Daan Wierstra. Matching Networks for One Shot Learning. In *Proceedings of the 30th Conference on the Advances in neural information processing systems*, 2016.
- [38] Jeffrey S Vitter. Random Sampling with a Reservoir. *ACM Transactions on Mathematical Software*, 11(1):37–57, 1985.
- [39] Felix Wiewel and Bin Yang. Entropy-Based Sample Selection for Online Continual Learning. In *Proceedings of the 28th European Signal Processing Conference*, pages 1477–1481, 2021. doi: 10.23919/Eusipco47968.2020.9287846.
- [40] Tongtong Wu, Massimo Caccia, Zhuang Li, Yuan-Fang Li, Guilin Qi, and Gholamreza Haffari. Pretrained Language Models in Continual Learning: A Comparative Study. In *Proceedings of the 10th International Conference on Learning Representations*, 2022.
- [41] Jaehong Yoon, Divyam Madaan, Eunho Yang, and Sung Ju Hwang. Online Coreset Selection for Rehearsal-based Continual Learning. In *Proceedings of the 10th International Conference on Learning Representations*, 2022.
- [42] Chen Zeno, Itay Golan, Elad Hoffer, and Daniel Soudry. Task Agnostic Continual Learning Using Online Variational Bayes. *arXiv preprint arXiv:1803.10123*, 2018.

A Reproducibility statement

To aid in the reproduction of our experiments, we provide a detailed explanation in Section 5.1 of the experimental setup and provide additional experimental details in Appendix F. Also, we provide the code used for the experiments in the supplementary material.

B Ethics statement

Continual Learning is a growing field and has the potential to have a large societal impact in the future. For example, a potential application of continual learning is for privacy-aware machine learning on mobile devices, where resource constraints mean that often a continual learning solution is necessary. Another example of the potential use of continual learning is for the adaptation of large models, as re-training large models from scratch when new data becomes available is expensive and environmentally costly, therefore continual learning methods may provide a way of updating these large models with minimal resource costs. So, this means that research in continual learning could have a positive impact on society, however it is also important to realise that without conscious effort continual learning may have negative impacts as well. For instance, when deploying continual learning in the real world, mitigating social bias will be a problem and importantly solutions proposed when using static datasets—for example, modifying the dataset in some way—are often not straightforwardly applicable in continual learning. Therefore, before continual learning methods can be used fully in the real world many problems, known and potentially unknown, need to be addressed but if through future research they are addressed, continual learning can have a positive societal impact.

C Limitations

We mention the limitations of DeepCCG throughout the paper. For example, we show that none of the methods, including DeepCCG, achieve performances close offline training performance for the task-incremental shifting window setting. This shows that there is much work to be done in this setting and for settings like it, where there is greater informational overlap between tasks, suggesting the need for new methods that are better at performing across task knowledge transfer. Also, we point out that we do not adapt our method when changing between task-incremental and class-incremental learning. This is notable as in DeepCCG there is no interaction between the mean parameters and associated Gaussians of classes that do not appear in the same task at training time and so it could be the case that some of these classes’ Gaussians significantly overlap, degrading performance in the class-incremental scenario. However, in our experiments this does not seem to be the case, but still a possible direction for future work would be to create a modification of DeepCCG that is specialised to class-incremental learning.

D Details of learning the embedding function

For DeepCCG, at time j , to compute the update to the embedding function f_{ϕ_j} , when given a batch D_j and a corresponding memory M_j , we proceed using the following steps. Firstly, we randomly sample $R_j \subset M_j$ of size r from memory. Then using only the other samples in memory, M_j/R_j , we compute the posterior density for each class mean— μ_c , with $c \in C$:

$$p(\mu_c|M_j/R_j) = p(\mu_c|M_{j,c}^z/R_j^z) \tag{12}$$

$$= \mathcal{N}\left(\mu_y|\overline{M_{j,c}^z/R_j^z}, \frac{1}{m-r}\mathbf{I}\right), \tag{13}$$

where $M_{j,c}^z = \{f_{\phi_j}(x)|(x, y) \in M_j \wedge y = c\}$ are the embeddings of points in the memory buffer with class y . R_j^z is defined likewise and we use the notation \overline{S} to denote the mean of the elements of a set S . Then we compute the posterior distribution of the embedded inputs $z \in D_j^z \cup R_j^z$ for each

class $c \in C$ utilizing

$$p(z|c, M_j/R_j) = p(z|c, M_{j,c}^z/R_j^z) \quad (14)$$

$$= \int p(z|c, \mu_c) p(\mu_c | M_{j,c}^z/R_j^z) d\mu_c \quad (15)$$

$$= \mathcal{N}\left(z | \overline{M_{j,c}^z/R_j^z}, \left(1 + \frac{1}{m-r}\right) \mathbf{I}\right). \quad (16)$$

Next, we compute the posterior predictive for each sample $(x, y) \in D_j \cup R_j$ with a task identifier $t_{(x,y)}$, which is known for samples in the current batch and is stored by our method for samples stored in memory, and where $z = f_{\phi_j}(x)$ using

$$p(y|z, t_{(x,y)}, M_j/R_j) = \frac{p(z|y, M_{j,y}^z/R_j^z) p(y|t_{(x,y)})}{\sum_{c \in C} p(z|Y=c, M_{j,c}^z/R_j^z) p(Y=c|t_{(x,y)})} \quad (17)$$

$$= \frac{p(z|y, M_{j,y}^z/R_j^z)}{\sum_{c \in C_{t_{(x,y)}}} p(z|Y=c, M_{j,c}^z/R_j^z)} \quad (18)$$

Finally, we update the embedding function by performing a gradient step using the formula

$$\phi_{j+1} = \phi_j + \eta \nabla_{\phi} \sum_{(x,y) \in D_j \cup R_j} \log(p(y|z = f_{\phi_j}(x), t_{(x,y)}, M_j/R_j)), \quad (19)$$

which can be seen as a per-sample log conditional marginal likelihood [24].

By using Eq. 16 and 18, the closed form of the posterior predictive distribution for a sample (x, y) with task identifier $t_{(x,y)}$ and where $z = f_{\phi_j}(x)$ is

$$p(y|z, t_{(x,y)}, M_j/R_j) = \frac{p(z|y, M_{j,y}^z/R_j^z)}{\sum_{c \in C_{t_{(x,y)}}} p(z|Y=c, M_{j,c}^z/R_j^z)} \quad (20)$$

$$= \frac{\mathcal{N}\left(z | \overline{M_{j,y}^z/R_j^z}, \left(1 + \frac{1}{m-r}\right) \mathbf{I}\right)}{\sum_{c \in C_{t_{(x,y)}}} \mathcal{N}\left(z | \overline{M_{j,c}^z/R_j^z}, \left(1 + \frac{1}{m-r}\right) \mathbf{I}\right)} \quad (21)$$

E Proof of robustness of sample selection mechanism to i.i.d. representation shift

We show that given a shift in representation that DeepCCG's sample selection mechanism maintains the property in expectation that it minimises the KL-Divergence between the posterior over the currently accessible data and the posterior induced by the samples selected to be store in memory. The proof is as follows: Let Z be the representation space and assume we are given a batch $D_{j,y}^Z =$ and memory $M_{j,y}^Z = \{f_{\phi}(x)|(x, y') \in M_j \wedge y' = y\}$ of data points in Z for a given class y . We define the representations shift as $z^* = z + \epsilon_z$ where $z \in D_{j,y}^Z \cup M_{j,y}^Z$ and ϵ_z is i.i.d. sampled from an arbitrary distribution with bounded mean and variance (i.e. $\mathbb{E}[\epsilon_z] < \infty$ and $\text{Var}(\epsilon_z) < \infty$). Furthermore, define $\nabla_z = \epsilon_z - \mathbb{E}[\epsilon_z]$, hence it is ϵ shifted to have zero mean. Additionally, let $D_{j,y}^{Z^*} = \{z^* = z + \epsilon_z | z \in D_{j,y}^Z\}$ and define $M_{j,y}^{Z^*}$ and $M_{j,y}'^{Z^*}$ likewise. Therefore we have that,

$$\mathbb{E}[\text{KL}(p(\mu_y | D_{j,y}^{Z^*}, M_{j,y}^{Z^*}) || p(\mu_y | M_{j,y}'^{Z^*}))] = \mathbb{E}[\|D_{j,y}^{Z^*} \cup M_{j,y}^{Z^*} - M_{j,y}'^{Z^*}\|_2^2] \quad (22)$$

$$= \mathbb{E}[\| \frac{1}{|D_{j,y}^{Z^*} \cup M_{j,y}^{Z^*}|} \sum_{z^* \in D_{j,y}^{Z^*} \cup M_{j,y}^{Z^*}} z^* - \frac{1}{|M_{j,y}'^{Z^*}|} \sum_{z^* \in M_{j,y}'^{Z^*}} z^* \|_2^2] \quad (23)$$

$$= \sum_{k=0}^d \mathbb{E}[\left(\frac{1}{|D_{j,y}^{Z^*} \cup M_{j,y}^{Z^*}|} \sum_{z^* \in D_{j,y}^{Z^*} \cup M_{j,y}^{Z^*}} z_k^* - \frac{1}{|M_{j,y}'^{Z^*}|} \sum_{z^* \in M_{j,y}'^{Z^*}} z_k^* \right)^2] \quad (24)$$

$$= \sum_{k=0}^d \mathbb{E}[\left(\frac{1}{|D_{j,y}^Z \cup M_{j,y}^Z|} \sum_{z \in D_{j,y}^Z \cup M_{j,y}^Z} (z_k + \mathbb{E}[\epsilon_{z,k}] + \eta_{z,k}) - \frac{1}{|M_{j,y}^Z|} \sum_{z \in M_{j,y}^Z} (z_k + \mathbb{E}[\epsilon_{z,k}] + \eta_{z,k}) \right)^2] \quad (25)$$

$$= \sum_{k=0}^d \mathbb{E} \left[\left(\frac{1}{|D_{j,y}^Z \cup M_{j,y}^Z|} \sum_{z \in D_{j,y}^Z \cup M_{j,y}^Z} (z_k + \eta_{z,k}) - \frac{1}{|M_y^{I'Z}|} \sum_{z \in M_y^{I'Z}} (z_k + \eta_{z,k}) \right) \right] \quad (26)$$

$$+ \left(\frac{1}{|D_{j,y}^Z \cup M_{j,y}^Z|} \sum_{z \in D_{j,y}^Z \cup M_{j,y}^Z} \mathbb{E}[\epsilon_{z,k}] - \frac{1}{|M_y^{I'Z}|} \sum_{z \in M_y^{I'Z}} \mathbb{E}[\epsilon_{z,k}] \right)^2 \quad (27)$$

$$= \sum_{k=0}^d \mathbb{E} \left[\left(\frac{1}{|D_{j,y}^Z \cup M_{j,y}^Z|} \sum_{z \in D_{j,y}^Z \cup M_{j,y}^Z} (z_k + \eta_{z,k}) - \frac{1}{|M_y^{I'Z}|} \sum_{z \in M_y^{I'Z}} (z_k + \eta_{z,k}) \right)^2 \right] \text{ (as } \epsilon_{z,k} \text{ are i.i.d)} \quad (28)$$

$$= \sum_{k=0}^d \mathbb{E} \left[\left(\frac{1}{|D_{j,y}^Z \cup M_{j,y}^Z|} \sum_{z \in D_{j,y}^Z \cup M_{j,y}^Z} z_k - \frac{1}{|M_y^{I'Z}|} \sum_{z \in M_y^{I'Z}} z_k \right) \right] \quad (29)$$

$$+ \frac{1}{|D_{j,y}^Z \cup M_{j,y}^Z|} \sum_{z \in D_{j,y}^Z \cup M_{j,y}^Z} \eta_{z,k} - \frac{1}{|M_y^{I'Z}|} \sum_{z \in M_y^{I'Z}} \eta_{z,k} \quad (30)$$

$$= \sum_{k=0}^d \mathbb{E} \left[\left(\frac{1}{|D_{j,y}^Z \cup M_{j,y}^Z|} \sum_{z \in D_{j,y}^Z \cup M_{j,y}^Z} z_k - \frac{1}{|M_y^{I'Z}|} \sum_{z \in M_y^{I'Z}} z_k \right)^2 \right] \quad (31)$$

$$+ 2\mathbb{E} \left[\left(\frac{1}{|D_{j,y}^Z \cup M_{j,y}^Z|} \sum_{z \in D_{j,y}^Z \cup M_{j,y}^Z} z_k - \frac{1}{|M_y^{I'Z}|} \sum_{z \in M_y^{I'Z}} z_k \right) \left(\frac{1}{|D_{j,y}^Z \cup M_{j,y}^Z|} \sum_{z \in D_{j,y}^Z \cup M_{j,y}^Z} \eta_{z,k} - \frac{1}{|M_y^{I'Z}|} \sum_{z \in M_y^{I'Z}} \eta_{z,k} \right) \right] \quad (32)$$

$$+ \mathbb{E} \left[\left(\frac{1}{|D_{j,y}^Z \cup M_{j,y}^Z|} \sum_{z \in D_{j,y}^Z \cup M_{j,y}^Z} \eta_{z,k} - \frac{1}{|M_y^{I'Z}|} \sum_{z \in M_y^{I'Z}} \eta_{z,k} \right)^2 \right] \quad (33)$$

$$= \sum_{k=0}^d \left(\frac{1}{|D_{j,y}^Z \cup M_{j,y}^Z|} \sum_{z \in D_{j,y}^Z \cup M_{j,y}^Z} z_k - \frac{1}{|M_y^{I'Z}|} \sum_{z \in M_y^{I'Z}} z_k \right)^2 \quad (34)$$

$$+ \sum_{k=0}^d \mathbb{E} \left[\left(\frac{1}{|D_{j,y}^Z \cup M_{j,y}^Z|} \sum_{z \in D_{j,y}^Z \cup M_{j,y}^Z} \eta_{z,k} - \frac{1}{|M_y^{I'Z}|} \sum_{z \in M_y^{I'Z}} \eta_{z,k} \right)^2 \right] \text{ (as } \mathbb{E}[\eta_{z,k}] = 0) \quad (35)$$

$$= \|\overline{D_{j,y}^Z \cup M_{j,y}^Z} - \overline{M_y^{I'Z}}\|_2^2 + \sum_{k=0}^d \left(\mathbb{E} \left[\left(\frac{1}{|D_{j,y}^Z \cup M_{j,y}^Z|} \sum_{z \in D_{j,y}^Z \cup M_{j,y}^Z} \eta_{z,k} \right)^2 \right] + \mathbb{E} \left[\left(\frac{1}{|M_y^{I'Z}|} \sum_{z \in M_y^{I'Z}} \eta_{z,k} \right)^2 \right] \right) \quad (36)$$

$$- 2\mathbb{E} \left[\left(\frac{1}{|D_{j,y}^Z \cup M_{j,y}^Z|} \sum_{z \in D_{j,y}^Z \cup M_{j,y}^Z} \eta_{z,k} \right) \left(\frac{1}{|M_y^{I'Z}|} \sum_{z \in M_y^{I'Z}} \eta_{z,k} \right) \right] \quad (37)$$

$$= \|\overline{D_{j,y}^Z \cup M_{j,y}^Z} - \overline{M_y^{I'Z}}\|_2^2 + \sum_{k=0}^d \left(\frac{\text{Var}(\epsilon_k)}{|D_{j,y}^Z \cup M_{j,y}^Z|} + \frac{\text{Var}(\epsilon_k)}{|M_y^{I'Z}|} \right) \quad (38)$$

$$- \frac{2}{|D_{j,y}^Z \cup M_{j,y}^Z| |M_y^{I'Z}|} \sum_{z \in D_{j,y}^Z \cup M_{j,y}^Z} \sum_{z' \in M_y^{I'Z}} \mathbb{E}[\eta_{z,k} \eta_{z',k}] \quad \text{(using formula for variance of means)} \quad (39)$$

$$= \|\overline{D_{j,y}^Z \cup M_{j,y}^Z} - \overline{M_y^{I'Z}}\|_2^2 + \left(\frac{1}{|D_{j,y}^Z \cup M_{j,y}^Z|} + \frac{1}{|M_y^{I'Z}|} \right) \sum_{k=0}^d \text{Var}(\epsilon_k) \quad (40)$$

$$+ \frac{2}{|D_{j,y}^Z \cup M_{j,y}^Z| |M_y^{I'Z}|} \sum_{k=0}^d \sum_{z \in M_y^{I'Z}} \mathbb{E}[\eta_{z,k}^2] \quad (41)$$

$$= \|\overline{D_{j,y}^Z \cup M_{j,y}^Z} - \overline{M_y^{I'Z}}\|_2^2 + \left(\frac{1}{|D_{j,y}^Z \cup M_{j,y}^Z|} + \frac{1}{|M_y^{I'Z}|}\right) \sum_{k=0}^d \text{Var}(\epsilon_k) - \frac{2}{|D_{j,y}^Z \cup M_{j,y}^Z|} \sum_{k=0}^d \text{Var}(\epsilon_k) \quad (42)$$

$$= \|\overline{D_{j,y}^Z \cup M_{j,y}^Z} - \overline{M_y^{I'Z}}\|_2^2 + \left(\frac{1}{|M_y^{I'Z}|} - \frac{1}{|D_{j,y}^Z \cup M_{j,y}^Z|}\right) \sum_{k=0}^d \text{Var}(\epsilon_k) \quad (43)$$

which completes the proof and where in the main paper we define $\nu = \sum_{k=0}^d \text{Var}(\epsilon_k)$.

F Additional experimental details

In addition to the experimental details mentioned in the main body of the paper, there are a few more details to mention. Firstly, for methods with hyperparameters we performed a grid search using the same experimental set up as the real experiments and 10% of the training data as validation data. This led to the selection of the hyperparameters of EWC and PackNet, the two methods with free hyperparameters, shown in Tables 4 and 5. Secondly, we use the same learning rate of 0.1 and the standard gradient decent optimiser for all methods. These were chosen by looking at the commonly selected values in previous work [27] and were shown to be performative for all methods tested. Lastly, for the multi-task upper bound we train using two epochs in the task-incremental scenario and three epochs in the class-incremental scenario, to more fairly upper bound the performance of the methods.

Table 4: Values selected for the hyperparameters of EWC and PackNet in the task-incremental learning experiments, which are the regularisation coefficient and the percentage of available filters to be used per task, respectively. SW stands for shifting window and DT stands for disjoint tasks.

Method	CIFAR-10		CIFAR-100		MiniImageNet	
	SW	DT	SW	DT	SW	DT
EWC	1	6	6	6	2	9
PackNet	0.3	0.3	0.1	0.1	0.05	0.2

Table 5: Values selected for the hyperparameters of EWC in the class-incremental learning experiments, which is the regularisation coefficient. SW stands for shifting window and DT stands for disjoint tasks.

Method	CIFAR-10		CIFAR-100		MiniImageNet	
	SW	DT	SW	DT	SW	DT
EWC	1	1	6	1	6	1

G Additional results

G.1 Results on using different memory sizes

One additional useful experiment is looking at the relationship between performance and the size of memory used for DeepCCG. Therefore, in Table 6 we show the performance of DeepCCG and the other replay methods compared against with varying memory size. Table 6 shows that when the memory size is increased to $m = 1250$, DeepCCG has an improvement in average accuracy relative to other methods, as it achieves 2.76% better than any other method for $m = 1250$, while for $m = 1000$ it achieves 2.57% better than any other method, a 0.19% improvement. When the memory size is decreased to $m = 750$, we see that DeepCCG’s performance drops more than other methods as it is only 0.25% better than other methods in this case. Therefore, our experiments show that compared to other replay methods DeepCCG’s performance increases the most when m increases and that for small buffer sizes DeepCCG performs less well, potentially due to the fact that the examples in the memory buffer are used to infer the posterior over the means of the per-class Gaussians and so

Table 6: Results of experiments looking at the effect of memory buffer size m for the replay methods tested, using the shifting window setting on CIFAR-100 in task-incremental learning scenario. We report mean average accuracy with their standard errors across three independent runs.

Method	m=750	m=1000	m=1250
ER-reservoir	53.17 \pm 0.656	54.05 \pm 0.626	55.22 \pm 0.592
A-GEM	27.18 \pm 1.091	29.01 \pm 1.449	27.87 \pm 0.172
EntropySS	50.52 \pm 0.725	51.80 \pm 0.700	53.34 \pm 0.372
GSS	47.15 \pm 0.766	48.20 \pm 0.332	46.18 \pm 0.341
DeepCCG (ours)	53.42\pm0.460	56.62\pm0.288	57.98\pm0.514

the method needs a given amount of examples to specify the means well. We also note that in our experiments the performance ranking of the methods does not change with m .

G.2 Additional representation shift results

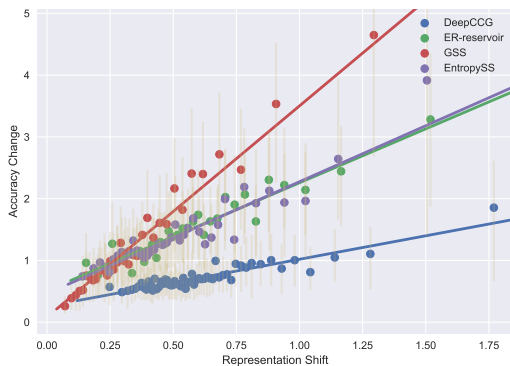


Figure 4: Binned scatter plot showing for the MiniImageNet disjoint tasks setting the change in accuracy against the mean change in representation after learning on a batch for the test data of the first task.